Available online at www.sciencedirect.com
ScienceDirect
Journal of Colloid and Interface Science 319 (2008) 429–434
JOURNAL OF Colloid and Interface Science
www.elsevier.com/locate/jcis

Enhancement of magnetic resonance contrast effect using ionic magnetic clusters

Sung-Baek Seo [a,b], Jaemoon Yang [b], Tong-Il Lee [c], Chan-Hwa Chung [d], Yong Jin Song [e], Jin-Suck Suh [a,f], Ho-Geun Yoon [g], Yong-Min Huh [a,f,*], Seungjoo Haam [a,b,*]

[a] *Graduate Program for Nanomedical Science, Yonsei University, Seoul 120-749, South Korea*
[b] *Department of Chemical Engineering, College of Engineering, Yonsei University, Seoul 120-749, South Korea*
[c] *ATGen, Advanced Technology Research Center, 68 Yatap-dong, Bundang-gu, Seongnam-si, Gyeonggi-do 463-816, South Korea*
[d] *Department of Chemical Engineering, Sungkyunkwan University, Suwon 440-746, South Korea*
[e] *Department of Physics, College of Natural Science, Ajou University, Suwon 433-749, South Korea*
[f] *Department of Radiology, College of Medicine, Yonsei University, Seoul 120-752, South Korea*
[g] *Department of Biochemistry and Molecular Biology, Center for Chronic Metabolic Disease Research, College of Medicine, Yonsei University, Seoul 120-752, South Korea*

Received 10 September 2007; accepted 19 November 2007

Available online 26 December 2007

Abstract

Precise diagnosis by magnetic resonance imaging (MRI) requires sensitive magnetic resonance probes to detect low concentrations of magnetic substances. Ionic magnetic clusters (IMCs) as versatile magnetic probes were successfully synthesized for enhancing the magnetic resonance (MR) contrast effect as well as ensuring high water solubility. IMCs with various sizes were prepared by assembly of MNCs using cationic cetyltrimethylammonium bromide (CTAB) and anionic sodium dodecyl sulfate (SDS). To synthesize IMCs in the aqueous phase, magnetic nanocrystals in an organic solvent were assembled with CTAB and SDS using the nanoemulsion method, to fabricate cationic magnetic clusters (CMCs) and anionic magnetic clusters (AMCs), respectively. IMCs demonstrated ultrasensitivity by MR imaging and sufficient magnetic mobility under an external magnetic field.

Keywords: Ionic magnetic clusters; Magnetic cluster size; MR contrast effect

1. Introduction

Magnetic resonance imaging (MRI) has been widely employed in medical diagnosis due to noninvasive applicability and excellent spatial resolution. Especially, magnetic nanoparticles as contrast agents have been developed for improving the diagnostic potentials because they could shorten spin–spin relaxation time (T2) and enhance MR images [1–4]. Recently, magnetic nanocrystals (MNCs) synthesized by the thermal decomposition method are considered as the most suitable material because of their high magnetic sensitivity [5]. In general, however, these MNCs are not readily applicable for MR contrast agents without an appropriate surface modification process to make them aqueous soluble because they are synthesized using organometallic precursors in an organic solvent. Thus, physicochemical techniques are being developed to prepare water-soluble MNCs such as layer-by-layer deposition using polyelectrolyte chains [6], surface-initiated polymerization [7,8], encapsulation process by amphiphilic polymers [9–11], and adsorption of charged ligands or stabilizers on surfaces of nanoparticles [12–14]. Among them, amphiphilic surfactants as phase transfer agents and stabilizers can formulate well-dispersed MNCs in water for MR contrast agents and clustering of MNCs can also be prepared and controlled by experimental conditions [15,16]. Moreover, recent research has reported that the MR signal could be significantly increased by the clustering of MNCs due to the enhanced magnetism [17–19].

* Corresponding authors. Faxes: +82 2 362 8647, +82 2 312 6401.
E-mail addresses: ymhuh@yuhs.ac.kr (Y.-M. Huh), haam@yonsei.ac.kr (S. Haam).

0021-9797/$ – see front matter
doi:10.1016/j.jcis.2007.11.026

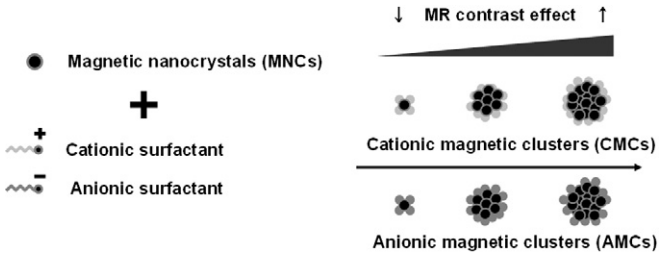

Fig. 1. Conceptual scheme of IMCs with various sizes by assembly of MNCs.

In this study, thus, we aimed to synthesize ionic magnetic clusters (IMCs) by assembly of MNCs using ionic surfactants for enhancement of the MR contrast effect and water solubility of MNCs. The cationic surface charge of magnetic nanoparticles can be a promising tool for stem cell labeling and tracking agents due to electrostatic interactions with negative charged cell membranes [20–22]. To fabricate gene delivery carriers, on the other hand, anionic surface charge of magnetic nanoparticles could easily be used for assembly with cationic substances without a complicated conjugation method [23,24]. Therefore, we prepared both cationic and anionic magnetic clusters using cetyltrimethylammonium bromide (CTAB) and sodium dodecyl sulfate (SDS), respectively. Fig. 1 shows the conceptual scheme of IMCs with various sizes by assembly of MNCs using both ionic surfactants. We evaluated the size, polydispersity, and the magnetic hysteresis loops of IMCs. Then, the amount of magnetic compounds in IMCs was measured by a thermogravimetric analyzer and the diagnostic potentials of IMCs as MR contrast agents were investigated by MRI.

2. Materials and methods

2.1. Materials

Iron chlorides, sodium oleate, oleic acid, 1-octadecene, cetyltrimethylammonium bromide, and sodium dodecyl sulfate were purchased from Sigma–Aldrich. Phosphate-buffered saline (PBS; 10 mM, pH 7.4) was purchased from Gibco. All other chemicals and reagents were of analytical grade.

2.2. Synthesis of magnetic nanocrystals

Fe_3O_4 nanocrystals were synthesized by thermal decomposition [25]. For the synthesis, 10.8 g of iron chloride and 36.5 g of sodium oleate were dissolved in a mixture solvent composed of ethanol (80 ml), distilled water (60 ml), and hexane (140 ml). The resulting mixture was heated to 70 °C and reacted for 4 h. When the reaction was completed, the upper organic layer containing the iron–oleate complex was washed three times with distilled water (30 ml) in a separatory funnel. After washing, hexane was evaporated off, resulting in an iron–oleate complex in a waxy solid form. The amounts of 36 g of the synthesized iron–oleate complex and 5.7 g of oleic acid were dissolved in 200 g of 1-octadecene at room temperature. The reaction mixture was heated to 320 °C with a constant heating rate of 3.3 °C min^{-1}, and then preserved for 30 min. The resulting solution containing the magnetic nanocrystals was then cooled to room temperature, and ethanol (500 ml) was added to the solution. MNCs were purified by centrifugation at 15,000 rpm.

2.3. Preparation of ionic magnetic clusters by the nanoemulsion method

10 mg of MNCs was dissolved in chloroform (4 ml), and then added to PBS (20 ml) containing 150, 75, and 50 mg of CTAB and SDS, respectively. After mutual saturation of the organic and the continuous phase, the mixture was emulsified for 10 min under ultrasonification (ULH700S, Ulssohitech) at 450 W [26]. After solvent evaporation, ionic magnetic clusters were purified by three cycles of centrifugation at 6800 rpm using a centrifugal filter (Amicon Ultra-15, Millipore).

2.4. MR imaging

MR imaging experiments were performed with a 1.5 T clinical MRI instrument with a Micro-47 surface coil (Intera, Philips Medical Systems). r_2 (T2 relaxivity coefficients with units of $mM^{-1}\,s^{-1}$) of IMCs containing magnetic nanocrystals were measured at room temperature by the Carr–Purcell–Meiboom–Gill (CPMG) sequence: TR = 10 s, 32 echoes with 12 ms even echo space, number of acquisitions = 1, point resolution of 156 × 156 μm, section thickness of 0.6 mm.

2.5. Characterization

Morphology and size were evaluated with a transmittance electron microscope (TEM, JEM-1011, JEOL Ltd.). Size distribution and surface charge of IMCs were analyzed by laser scattering (ELS-Z, Otsuka electronics). FTIR spectra (Excalibur series, Varian Inc.) analysis was performed to confirm the characteristic bands of the synthesized clusters. The quantity of magnetic compounds in IMCs was determined by a thermogravimetric analyzer (SDT-Q600, TA instrument). The saturation of magnetization was evaluated using a vibrating-sample magnetometer (VSM, Model 7300, Lakeshore). The amount of metals and nonmetals in IMCs was determined by inductively coupled plasma mass spectrometry (ICP-MS, Optima 4300DU, VG Elemental Ltd.).

3. Results and discussion

Monodispersed magnetic nanocrystals were synthesized in an organic solvent for magnetic components of MRI contrast agents. The TEM image of MNCs, shown in Fig. 2a, exhibited a spherical morphology of uniform 9 nm nanocrystals, demonstrating their narrow particle-size distribution (size variation = 5.2%). High-resolution TEM (HRTEM) image of MNCs showed distinct lattice fringe patterns, indicating the highly crystalline nature of the nanocrystals (Fig. 2b). To evaluate the magnetic sensitivity of the MNCs under a magnetic field, the magnetic moment was analyzed using a vibrating sample magnetometer (VSM). The hysteresis loop of MNCs observed at

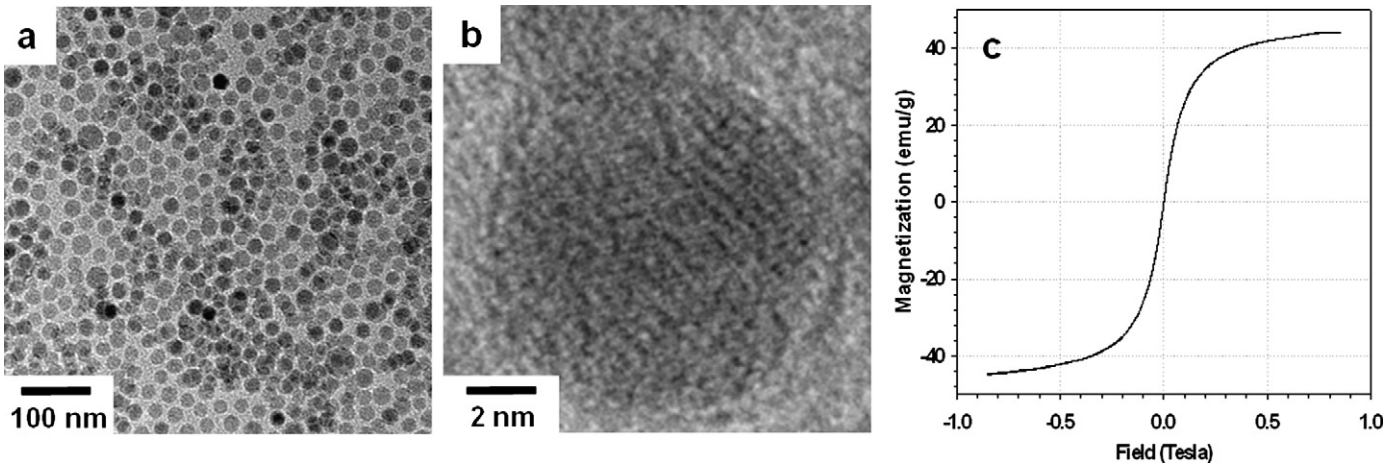

Fig. 2. (a) TEM image, (b) HRTEM image, and (c) magnetic hysteresis loops of MNCs.

Table 1
Experimental conditions for preparing IMCs

IMCs	Ionic surfactants (mg/ml)		MNCs (mg/ml)
	CTAB	SDS	
CMC-1	7.50	0	2.50
CMC-2	3.75	0	2.50
CMC-3	2.50	0	2.50
AMC-1	0	7.50	2.50
AMC-2	0	3.75	2.50
AMC-3	0	2.50	2.50

300 K exhibited a superparamagnetic behavior without magnetic hysteresis (Fig. 2c). The saturation of magnetization value of MNCs at 0.9 T was 44.3 emu/g.

To synthesize ionic magnetic clusters stabilized in the aqueous phase, MNCs in an organic solvent were assembled with CTAB and SDS using the nanoemulsion method, to fabricate cationic magnetic clusters (CMCs) and anionic magnetic clusters (AMCs), respectively. Individual hydrophobic MNCs thermodynamically tend to render IMCs in water, because the solvation free energy of clusters is lower than the overall solvation free energy of individual hydrophobic particles [27]. Table 1 presents the experimental conditions for preparing IMCs. Fig. 3a shows MNCs dissolved in chloroform (bottom of the two-phase mixture) and IMCs well dispersed in PBS after phase transfer (top of the two-phase mixture) due to electrostatic repulsion between IMCs. The narrow size distribution and polydispersity (PDI = 0.25–0.32) of IMCs were measured by laser scattering (Fig. 3b). The decrease in size of IMCs was observed with increasing concentration of CTAB and SDS. It is considered that excess surfactants are required for stabilization of the smaller emulsion droplets created under ultrasonication [28]. Moreover, the sizes of CMCs were larger than those of AMCs at the same concentration of surfactants. The result is attributed to the fact that formation of CMCs is easier than that of AMCs due to the lower critical micelle concentration of CTAB [29,30]. In Fig. 3c, zeta potential values of CMCs and AMCs were found in the range of 15.2–21.1 and −10.8–−7.8 mV, respectively. CMCs and AMCs maintained stable zeta potential values under various weight ratios of ionic surfactant/MNCs. These data indicated that the colloidal stability of IMCs was successfully achieved by assembly of MNCs with ionic surfactants.

TEM images of CMCs and AMCs are shown in Fig. 4. The prepared CMCs and AMCs have a uniformly spherical shape but different magnetic cluster size according to the concentration of surfactants during the synthetic process. As shown in Fig. 5, the saturation of magnetization values of CMC-1, CMC-2, CMC-3, AMC-1, AMC-2, and AMC-3 at 0.9 T were 10.9, 14.8, 23.5, 12.6, 16.3, and 25.6 emu/g, respectively. The values of CMCs and AMCs were lower than those of MNCs (44.3 emu/g) due to the presence of organic components (CATB and SDS). The amounts of magnetic compounds in CMC-1, CMC-2, CMC-3, AMC-1, AMC-2, and AMC-3 were determined to be 16, 28, 46, 25, 33, and 50 wt% using a thermogravimetric analyzer, respectively (Fig. 6). The Fe elemental-based saturation of magnetization of CMCs and AMCs was similar to that of pure magnetic nanocrystals. From the above saturation of magnetization values and the quantity of magnetic compounds in CMCs and AMCs, we demonstrated that tunable magnetic cluster size could be obtained by controlling the concentration of ionic surfactant resulting from assembly between ionic surfactants and MNCs.

The presence of the MNCs and organic components (CTAB and SDS) in IMCs was confirmed by FTIR spectra (Fig. 7). The characteristic bands of CTAB in CMCs at 1500 cm^{-1} (N–H bend) and 1400 cm^{-1} (C–N stretch) and SDS in AMCs at 1200 cm^{-1} (S=O), 1000 cm^{-1} (S–O), and 850 cm^{-1} (S–O) were observed. After IMCs were prepared, a band was presented at 550 cm^{-1} (Fe–O) dependent on the Fe(II) content in the CMCs and AMCs.

We also investigated the MR contrast effect of IMCs by measuring their r_2 (T2 relaxivity coefficients) to confirm their utility as MRI contrast agents. At 1.5 T, the r_2 values of IMCs increased obviously with increasing magnetic cluster size (Fig. 8). The r_2 started at 112.5 $mM^{-1}\,s^{-1}$ for CMC-1, increased to 135.2 $mM^{-1}\,s^{-1}$ for CMC-2, and culminated at 227.6 $mM^{-1}\,s^{-1}$ for CMC-3. Likewise, the r_2 started at 115.6 $mM^{-1}\,s^{-1}$ for AMC-1, increased to 146.8 $mM^{-1}\,s^{-1}$ for AMC-2, and culminated at 223.5 $mM^{-1}\,s^{-1}$ for AMC-3. As a

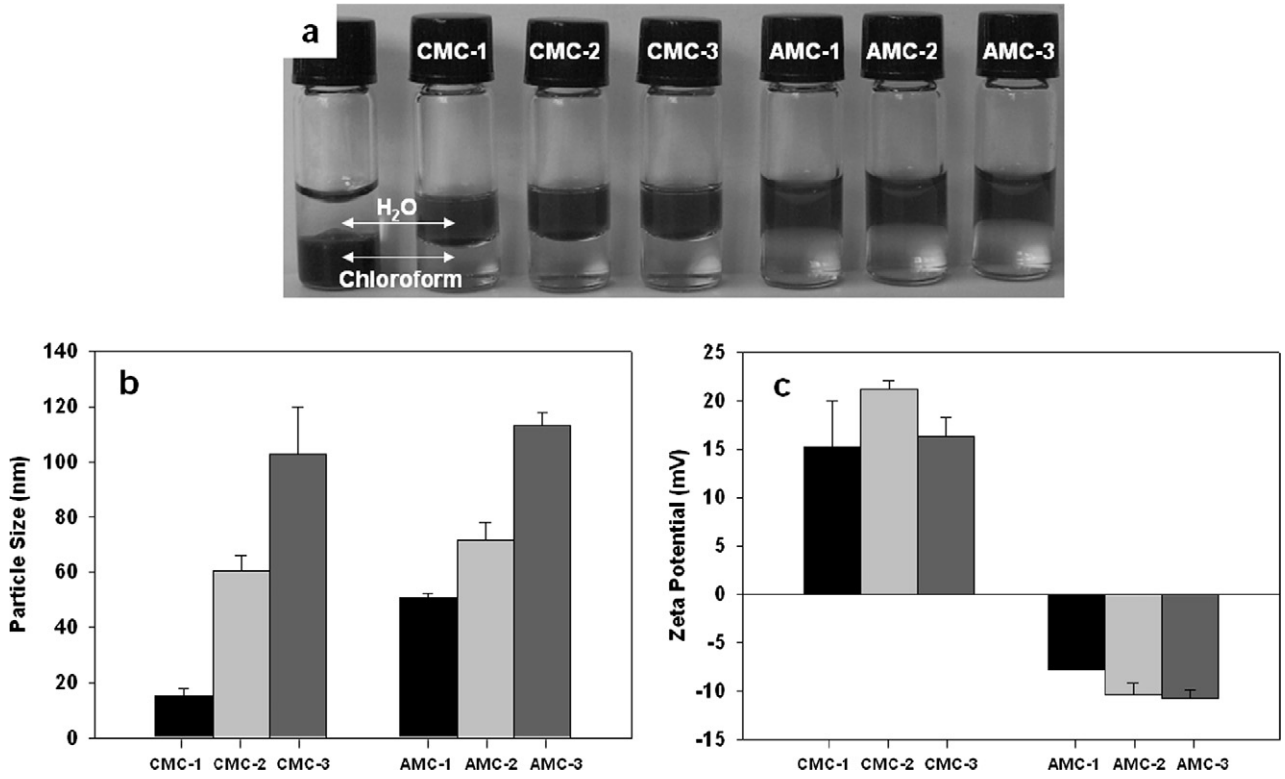

Fig. 3. (a) Photograph of two-phase mixtures with MNCs dissolved in chloroform (the left side) and IMCs dispersed in PBS after phase transfer. (b) Particle size and (c) surface charge of CMCs and AMCs according to surfactant/MNCs ratio.

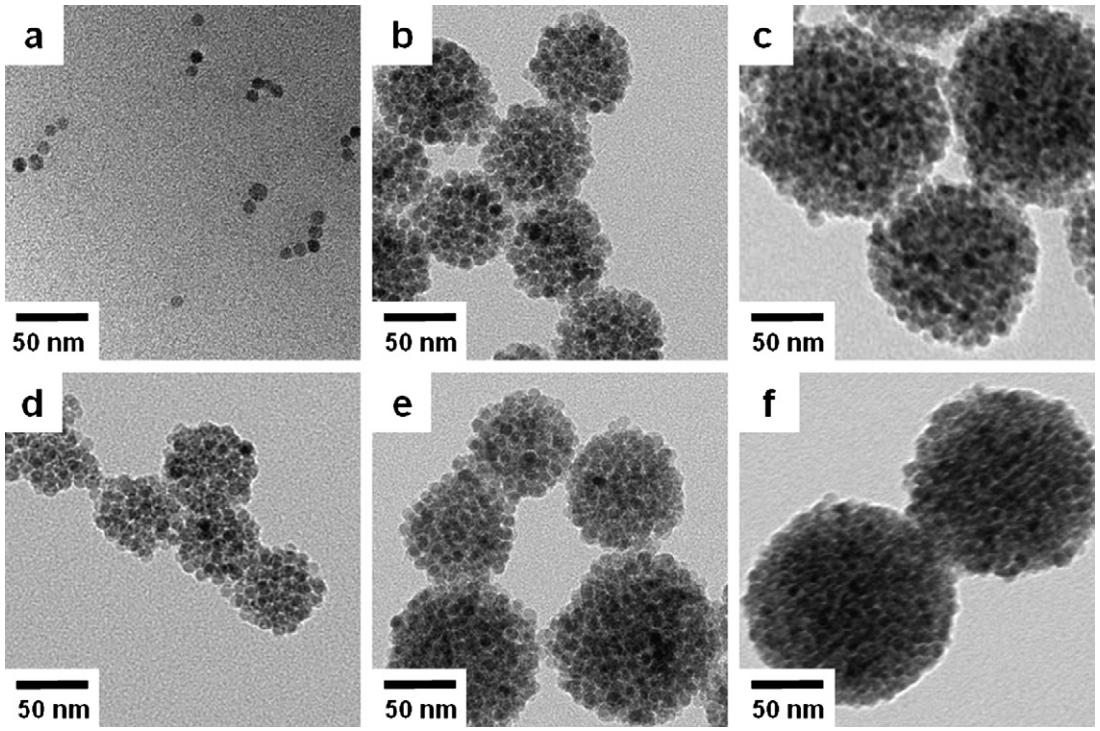

Fig. 4. TEM images of (a) CMC-1, (b) CMC-2, (c) CMC-3, (d) AMC-1, (e) AMC-2, and (f) AMC-3.

result, the CMC-3 and AMC-3 provide remarkably dark MR contrasts of an approximate 2.02-fold and 1.93-fold increased r_2 values compared to those of CMC-1 and AMC-1. Such a significant improvement in the MR signal was attributed to the enhanced magnetism of multiple clustering of MNCs [17–19]. Furthermore, these results demonstrated that the CMCs and AMCs as MR imaging probes possessed sufficient magnetic properties for molecular imaging.

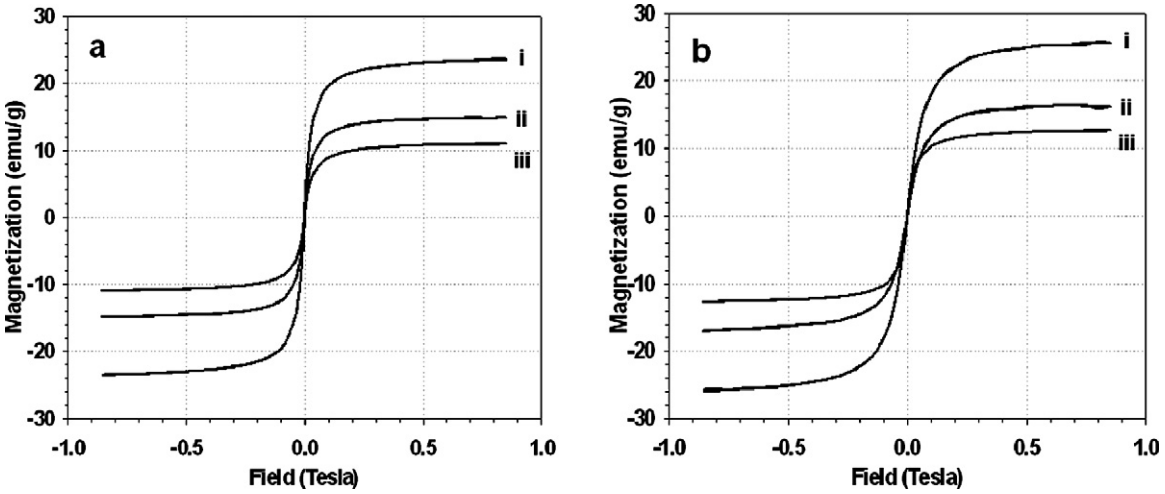

Fig. 5. Magnetic hysteresis loops using a vibrating sample magnetometer; (a) CMCs ((i) CMC-3, (ii) CMC-2, (iii) CMC-1) and (b) AMCs ((i) AMC-3, (ii) AMC-2, (iii) AMC-1).

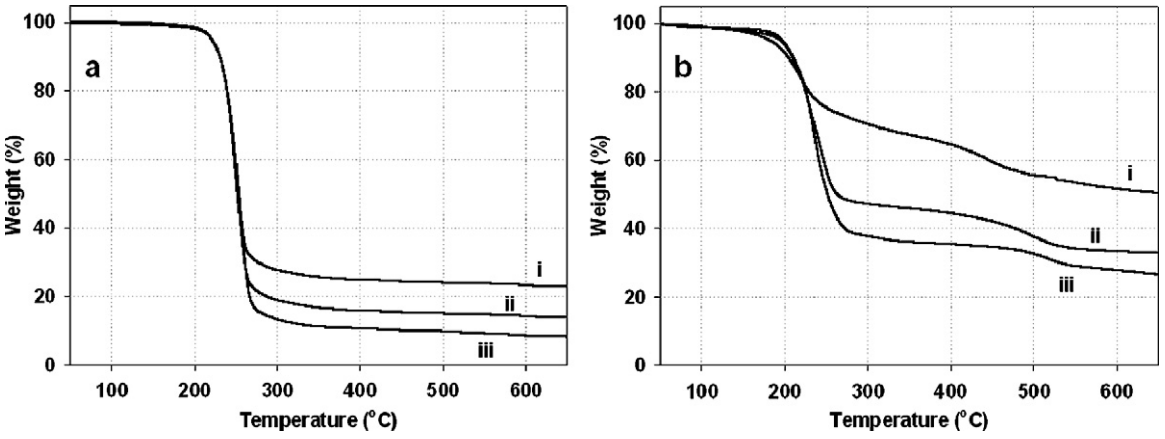

Fig. 6. Thermogravimetric curve of (a) CMCs ((i) CMC-3, (ii) CMC-2, (iii) CMC-1) and (b) AMCs ((i) AMC-3, (ii) AMC-2, (iii) AMC-1).

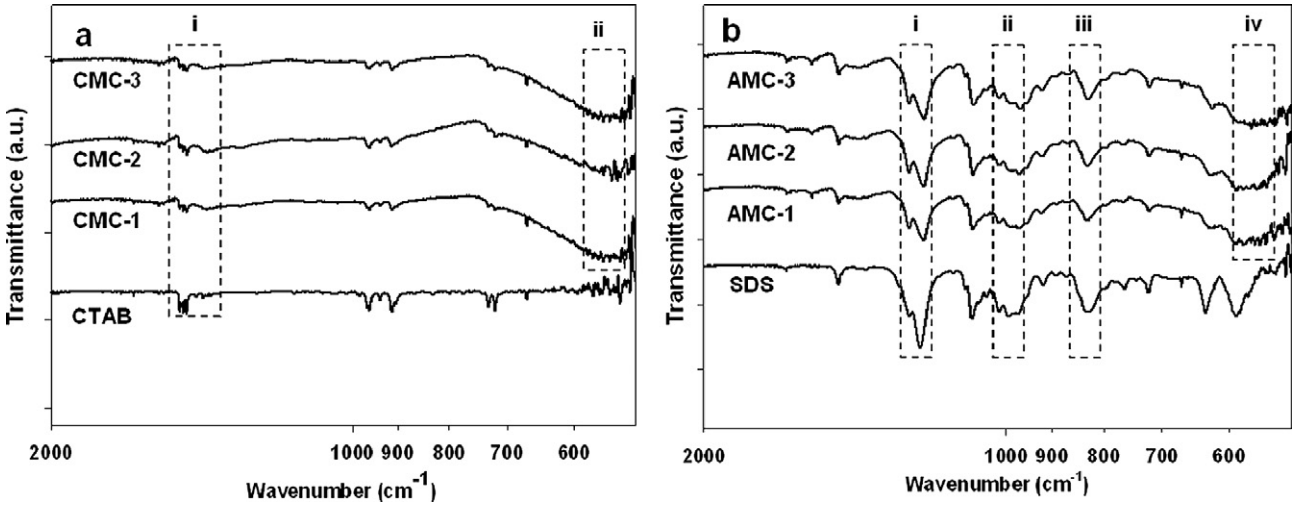

Fig. 7. FT-IR spectra of (a) CMCs ((i) N–H bend and C–N stretch, (ii) Fe–O) and (b) AMCs ((i) S=O, (ii) S–O, (iii) S–O, (iv) Fe–O).

4. Summary

We successfully synthesized ionic magnetic clusters with various sizes by assembly of MNCs with charged surfactants for enhancing the MR contrast effect as well as ensuring high water solubility of MNCs. Cationic and anionic magnetic clusters (CMCs and AMCs) exhibited sufficient magnetic properties applicable as ultrasensitive MR imaging contrast agents.

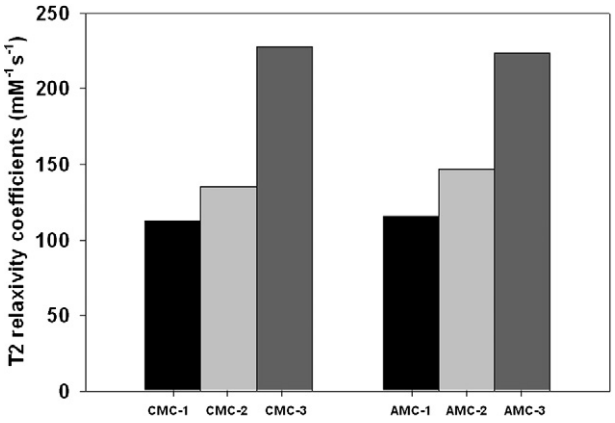

Fig. 8. Graph of T2 relaxivity coefficients (1/T2 versus the iron concentration) in the CMCs and AMCs.

Moreover, we enhanced the MR contrast effect with improved sensitivity of the MR signal by controlling the magnetic cluster size.

Acknowledgments

This work was supported by Korea Science and Engineering Foundation (KOSEF) (R15-2004-024-00000-0, No. M10755020001-07N5502-00110 and 2006-04649).

References

[1] L. Josephson, J. Lewis, P. Jacobs, P.F. Hahn, D.D. Stark, Magn. Reson. Imag. 6 (1988) 647–653.
[2] L. Josephson, C.H. Tung, A. Moore, R. Weissleder, Bioconj. Chem. 10 (2) (1999) 186–191.
[3] R. Weissleder, A. Moore, U. Mahmood, R. Bhorade, H. Benveniste, E.A. Chiocca, J.P. Basilion, Nat. Med. 6 (3) (2000) 351–355.
[4] M. Zhao, D.A. Beauregard, L. Loizou, B. Davletov, K.M. Brindle, Nat. Med. 7 (11) (2001) 1241–1244.
[5] J.-H. Lee, Y.-M. Huh, Y.-W. Jun, J.-W. Seo, J.-T. Jang, H.-T. Song, S. Kim, E.-J. Cho, H.-G. Yoon, J.-S. Suh, J. Cheon, Nat. Med. 13 (1) (2007) 95–99.
[6] F. Caruso, R.A. Caruso, H. Mohwald, Science 282 (1998) 1111–1114.
[7] H. Ohno, K.M. Koh, Y. Tsuji, T. Fukuda, Macromolecules 35 (24) (2002) 8989–8993.
[8] Y. Wang, X. Teng, J.S. Wang, H. Yang, Nano Lett. 3 (6) (2003) 789–793.
[9] J.J. Chiu, B.J. Kim, E.J. Kramer, D.J. Pine, J. Am. Chem. Soc. 127 (14) (2005) 5036–5037.
[10] V. Salgueiriño-Maceira, L.M. Liz-Marzán, M. Farle, Langmuir 20 (16) (2004) 6946–6950.
[11] J.-F. Berret, N. Schonbeck, F. Gazeau, D. El-Kharrat, O. Sandre, A. Vacher, M. Airiau, J. Am. Chem. Soc. 128 (2006) 1755–1761.
[12] J.N. Cha, H. Birkedal, L.E. Euliss, M.H. Bartl, M.S. Wong, T.J. Deming, G.D. Stucky, J. Am. Chem. Soc. 125 (27) (2003) 8285–8289.
[13] H. Mori, M.G. Lanzendorfer, A.H.E. Muller, J.E. Klee, Langmuir 20 (5) (2004) 1934–1944.
[14] A. Sehgal, Y. Lalatonne, J.F. Berret, M. Morvan, Langmuir 21 (20) (2005) 9359–9364.
[15] M. Gaumet, R. Gurny, F. Delie, Int. J. Pharm. 342 (2007) 222–230.
[16] M. Lee, Y.W. Cho, J.H. Park, H. Chung, S.Y. Jeong, K. Choi, D.H. Moon, S.Y. Kim, I.-S. Kim, I.C. Kwon, Colloid Polym. Sci. 284 (5) (2006) 506–512.
[17] A. Roch, Y. Gossuin, R.N. Muller, P. Gillis, J. Magn. Magn. Mater. 293 (2005) 532–539.
[18] J.M. Perez, L. Josephson, T. O'Loughlin, D. Hogemann, R. Weissleder, Nat. Biotechnol. 20 (2002) 816–820.
[19] H. Ai, C. Flask, B. Weinberg, X. Shuai, M. Pagel, D. Farrell, J. Duerk, J. Gao, Adv. Mater. 17 (2005) 1949–1952.
[20] H. Song, J. Choi, Y. Huh, S. Kim, Y. Jun, J. Suh, J. Cheon, J. Am. Chem. Soc. 127 (28) (2005) 9992–9993.
[21] A. Ito, E. Hibino, H. Honda, K. Hata, H. Kagamic, M. Uedad, T. Kobayashi, Biochem. Eng. J. 20 (2004) 119–125.
[22] A.S. Arbab, L.A. Bashaw, B.R. Miller, E.K. Jordan, B.K. Lewis, H. Kalish, J.A. Frank, Radiology 229 (3) (2003) 838–846.
[23] N. Nishiyama, A. Iriyama, W. Jang, K. Miyata, K. Itaka, Y. Inoue, H. Takahashi, Y. Yanagi, Y. Tamaki, H. Koyama, K. Kataoka, Nat. Mater. 4 (2005) 934–941.
[24] A.K. Gupta, M. Gupta, Biomaterials 26 (2005) 3995–4021.
[25] J. Park, K. An, Y. Hwang, J. Park, H. Noh, J. Kim, J. Park, N. Hwang, T. Hyeon, Nat. Mater. 3 (2004) 891–895.
[26] J. Yang, C. Lee, J. Park, S. Seo, E. Lim, Y. Song, J.S. Suh, H. Yoon, Y. Huh, S. Haam, J. Mater. Chem. 17 (2007) 2695–2699.
[27] D. Chandler, Nature 437 (29) (2005) 640–647.
[28] C.E. Astete, C.S.S.R. Kumar, C.M. Sabliov, Colloids Surf. A 299 (2007) 209–216.
[29] C. Vautier-Giongo, H.O. Pastore, J. Colloid Interface Sci. 299 (2006) 874–882.
[30] S. Desgouilles, C. Vauthier, D. Bazile, J. Vacus, J.-L. Grossiord, M. Veillard, P. Couvreur, Langmuir 19 (2003) 9504–9510.